Biomaterials 34 (2013) 4612–4621

Contents lists available at SciVerse ScienceDirect

Biomaterials

journal homepage: www.elsevier.com/locate/biomaterials

Mapping calcium phosphate activated gene networks as a strategy for targeted osteoinduction of human progenitors

Jeroen Eyckmans [a,c,d,1], Scott J. Roberts [a,c,1], Johanna Bolander [a,c], Jan Schrooten [b,c], Christopher S. Chen [d], Frank P. Luyten [a,c,*]

[a] Skeletal Biology and Engineering Research Center, Department of Development and Regeneration, KU Leuven, O&N1, Herestraat 49, PB 813, 3000 Leuven, Belgium
[b] Department of Metallurgy and Materials Engineering, KU Leuven, Kasteelpark Arenberg 44, PB 2450, 3001 Leuven, Belgium
[c] Prometheus, Division of Skeletal Tissue Engineering, KU Leuven, O&N 1, Herestraat 49, PB 813, B-3000 Leuven, Belgium
[d] Department of Bioengineering, University of Pennsylvania, 510 Skirkanich Hall, 210 South 33rd Street, Philadelphia, PA 19104, USA

ARTICLE INFO

Article history:
Received 8 January 2013
Accepted 5 March 2013
Available online 26 March 2013

Keywords:
Calcium phosphate
Bone tissue engineering
Gene expression
Osteogenesis
Progenitor cell

ABSTRACT

Although calcium phosphate-containing biomaterials are promising scaffolds for bone regenerative strategies, the osteoinductive capacity of such materials is poorly understood. In this study, we investigated whether endogenous mechanisms of *in vivo* calcium phosphate-driven, ectopic bone formation could be identified and used to induce enhanced differentiation *in vitro* of the same progenitor population. To accomplish this, human periosteum derived cells (hPDCs) were seeded on hydroxyapatite/collagen scaffolds (calcium phosphate rich matrix or CPRM), or on decalcified scaffolds (calcium phosphate depleted matrix or CPDM), followed by subcutaneous implantation in nude mice to trigger ectopic bone formation. In this system, osteoblast differentiation occurred in CPRM scaffolds, but not in CPDM scaffolds. Gene expression was assessed by human full-genome microarray at 20 h after seeding, and 2, 8 and 18 days after implantation. In both matrices, implantation of the cell constructs triggered a similar gene expression cascade, however, gene expression dynamics progressed faster in CPRM scaffolds than in CPDM scaffolds. The difference in gene expression dynamics was associated with differential activation of hub genes and molecular signaling pathways related to calcium signaling (CREB), inflammation (TNFα, NFkB, and IL6) and bone development (TGFβ, β-catenin, BMP, EGF, and ERK signaling). Starting from this set of pathways, a growth factor cocktail was developed that robustly enhanced osteogenesis *in vitro* and *in vivo*. Taken together, our data demonstrate that through the identification and subsequent stimulation of genes, proteins and signaling pathways associated with calcium phosphate mediated osteoinduction, a focused approach to develop targeted differentiation protocols in adult progenitor cells can be achieved.

1. Introduction

The combination of calcium phosphate (CaP)-containing biomaterials and osteogenic adult progenitors has been heralded as a promising tissue engineered solution for skeletal regeneration. Indeed, human MSCs derived from bone marrow [1], adipose tissue [2], cartilage [3], synovium [4], and periosteum [5] have the capacity to fully develop into osteoblasts and form mature bone tissue when they are seeded on CaP scaffolds and implanted ectopically in mice. However, factors attributing to the activation and differentiation of the implanted cells remain unclear. It is also unknown if additional non-autonomous factors such as host cell or environmental participation is required for tissue formation. Nevertheless, much research is being conducted on the manipulation of the physico-chemical and structural properties of these materials to optimize *in vivo* tissue formation, without information on how these properties exert their biological effect. This 'trial and error' approach to produce laboratory derived tissues has culminated in little clinically relevant progress being made since the dawn of the Tissue Engineering concept in 1993 [6]. This has led to novel paradigms such as "Developmental Engineering" being formulated [7]. Fundamentally, this concept prescribes that the closer the engineering is in relation to developmental or postnatal processes, the higher the success rate will be.

During development and postnatal homeostasis the formation of the CaP (carbonate apatite) component of bone tissue is initiated

* Corresponding author. Skeletal Biology and Engineering Research Center, KU Leuven, O&N1, Herestraat 49, PB 813, 3000 Leuven, Belgium. Tel.: +32 16 34 25 41; fax: +32 16 34 25 43.
E-mail address: Frank.Luyten@uz.kuleuven.be (F.P. Luyten).
[1] These authors have contributed equally to this work.

0142-9612/$ – see front matter © 2013 Elsevier Ltd. All rights reserved.
http://dx.doi.org/10.1016/j.biomaterials.2013.03.011

by osteoblasts. This process is mediated through the cellular production of a matrix which is permissible to nucleation and growth of hydroxyapatite crystals from Ca^{2+} and PO_4^{3-} (Pi) ions. It has been proposed that the release of this inorganic phase, during bone remodeling, is responsible for the differentiation of osteoprogenitors in the microenvironment, a notion that has been partially confirmed using CaP containing biomaterials [8]. We have previously attempted to deduce whether administration of Ca^{2+} and Pi *in vitro* is sufficient to modulate osteogenic differentiation [9] and *in vivo* tissue formation from human periosteum derived cells (hPDCs) [10], the cell type known to mediate postnatal fracture repair [11]. Although a number of osteogenic markers, including Bone Morphogenetic Protein 2 (BMP2), Osteocalcin (OCN) and Osteopontin (OPN), were found to be regulated *in vitro* by Ca^{2+} and Pi, the regulation of Runx2, a key osteogenic transcription factor, was limited. It has recently been reported that MAPK signaling may, in part, mediate this effect as MEK1/2 inhibition abrogated Ca^{2+} induced BMP2 expression [12]. Furthermore, it has been suggested that the *in vitro* regulation of OCN by CaP may be attributed to cells attempting to control the concentration of Ca^{2+} ions in culture medium [13]. Although these studies outline *in vitro* effects of Ca^{2+} ions, the relationship of this to *in vivo* osteoinduction by CaP biomaterials remains un-tested.

In an attempt to define the mechanisms of osteoinduction by CaP *in vivo*, we have previously developed a model system in which CaP carrier structures (Collagraft™) were decalcified, resulting in an abrogation of *in vivo* bone formation [14]. Herein, we hypothesize that CaP may initialize osteogenic gene networks in hPDCs shortly after implantation. To address this hypothesis, we examine genome-wide gene expression signatures of hPDCs engrafted on decalcified and non-decalcified Collagraft™ carriers before and after subcutaneous implantation in nude mice. We propose that through bioinformatics and phosphorylated protein analysis, gene networks and signaling pathways, which are differentially activated over time between decalcified and non-decalcified matrices, can be identified. We subsequently explore whether activation of these signaling pathways with soluble factors promote osteogenic differentiation *in vitro* and if predifferentiation of hPDCs in this manner would impact bone formation post-implantation.

2. Materials and methods

2.1. Cell culture

Periosteum was harvested from patients and periosteal cells were enzymatically released from the matrix. Tissue culture plastic adherent cells were expanded in DMEM medium supplemented with 10% fetal bovine serum as described previously [14]. HPDC from three donors were used for the microarray experiment, a pool of 6 donors was utilized to optimize the osteogenic growth factor cocktail (GFC) and the validation of the GFC was evaluated on hPDCs from four different donors. For *in vitro* osteogenic differentiation assays, passage 6 to 9 hPDCs were seeded at 3000 cells/cm^2 in either 96-well plates to assess proliferation and alkaline phosphatase activity or in 24-well plates for quantifying gene expression. Medium was changed every other day. Supplemental factors were TNFα, IL6 (R&D Systems, Minneapolis, MN), TGFβ1 (Stem Cell Research, CA), Ascorbic Acid (Sigma, St.Louis, MO), Ca^{2+} and Pi. Calcium and phosphate ion working solutions were prepared as described in Ref. [9]. Control cells were treated with either growth medium or osteogenic medium (OM) containing dexamethasone, Ascorbic Acid and β-glycerophosphate (hMSC Osteogenic BulletKit, Lonza).

2.2. Preparation of the scaffolds

Collagraft™ (Neucoll Inc., Cambell, California, US), an open porous composite made of CaP granules consisting of 65% hydroxyapatite (HA) and 35% β- tri-calcium phosphate (β-TCP), embedded in a bovine collagen type I matrix, was punched into 21 mm^3 cylindrical (diameter 3 mm, height 3 mm) scaffolds. Half of the Collagraft™ scaffolds were immersed in an EDTA/PBS buffer for two weeks to reduce the amount of CaP. Control scaffolds were left untreated. After treatment, the scaffolds were washed twice with PBS followed by lyophilization to dry the structures. CaP depletion was confirmed by microfocus computed tomography (Fig. S1). In the text, we annotate Collagraft™ and decalcified Collagraft™ with CPRM (calcium phosphate rich matrices) and CPDM (calcium phosphate depleted matrices) respectively.

2.3. In vivo osteogenesis

Passage three human periosteum-derived cells (hPDCs) were trypsin released, centrifuged and re-suspended at a concentration of 20 million cells/ml. One million cells were drop seeded on the upper surface of each scaffold (CPRM or CPDM) or replated in a T175 flask (2D reference condition) and incubated overnight at 37 °C to allow cell attachment. After incubation, the cell-seeded scaffolds were directly implanted subcutaneously in the back at the cervical region of NMRI-*nu/nu* mice. All procedures were approved by the local ethical committee for Animal Research (KU Leuven). The animals were housed according to the guidelines of the Animalium Leuven (KU Leuven).

2.4. RNA extraction and microarray analysis

Twenty hours after seeding (*in vitro*) and 2, 8 and 18 days after implantation (*in vivo*) implants were harvested, flash frozen in liquid nitrogen, homogenized (Ingenieurbüro CAT M. Zipperer GmbH, Staufen, Germany) and processed for RNA extraction with the fibrous mini RNA extraction kit (Qiagen, Venlo, Netherlands) according to the manufacturer's procedures. The microarrays were processed by the Micro Array Facility of the VIB (Flemish Institute of Biotechnology, Leuven, Belgium). Briefly, 1 μg of RNA from each sample that passed the Quality Control as determined by band densitometry of ribosomal RNA was spotted on Agilent Single Color Human MicroArray Chips (Agilent H44K). Fluorescent intensities were measured, converted into Log2 values and corrected for background signal. To allow comparison of gene expression across different arrays, a quantile normalization of the data was performed using the Agilent Feature Extraction software. Differential gene expression between two consecutive time points, or between the CPRM and CPDM scaffolds, was determined by a *t*-test with a cut-off of uncorrected *p*-value of $p < 0.001$.

2.5. Selection of gene of interest (GOI) and bioinformatics analysis

A GOI was defined as a gene which was differentially expressed between two consecutive time points in the Collagraft™ condition, but not in the decalcified condition **and** which was differentially expressed between the two conditions at the latter time point (cut-off: $p < 0.001$). After removing duplicate probes and unknown ID's the list of GOI contained 946 genes (Table S1).

Gene ontology was performed with DAVID (Database for Annotation, Visualization and Integrated Discovery, http://david.abcc.ncifcrf.gov/) to discover the main biological processes at each time point. The stringency for functional clustering was set on "high" [15].

Gene topology of the GOI list was visualized with Gene Expression Dynamics Inspector [16]. The parameter settings to generate Self Organizing Maps (SOMs) with a grid size of 11 by 12 tiles were for first/second phase 80/160 iterations with neighborhood radius 4/1, learning factor 0.6/0.1, conscience 5/5 and neighborhood block size 2/1. The data was linearly initialized with random seed set to 1 and the tiles were arranged according to Euclidean Distance. Clustering of co-expressed genes was performed utilizing GEDI with the "Neighborhood block Size" parameter set to 1 in the first training phase [16]. 110 Clusters with an average gene size of 11 (±6) genes per cluster were obtained. For each cluster, the average gene expression and standard deviation for every time point was calculated and statistically compared between CPRM and CPDM. Clusters having no significant differences at any time point were omitted from further analysis (student *t*-test, *p*-value cut-off $p < 0.001$). The remaining 64 clusters were ranked according to their *p*-value starting with the lowest *p*-value first. The first 32 clusters (representing 553 genes or 58% of the GOI list) were used for subsequent analysis. Temporal profiles of the metagenes (=average expression of the genes within a cluster) were plotted for each of the 32 clusters, and could be organized in 6 superclusters (Fig. S2). Genes from each supercluster were loaded in Ingenuity Pathway Analysis (Ingenuity Systems, Redwood City, California) for gene network reconstruction. Gene networks were built with a restriction of 70 genes per network and 25 networks per supercluster (Table S2).

2.6. Quantitative PCR

Complementary DNA (cDNA) was obtained by reverse transcription of 1 μg of total RNA with Oligo (dT) 20 as primer (Superscript III; Invitrogen, Merelbeke, Belgium). Sybr Green PCR was performed in 10 μl reactions in a Rotor-Gene-Q (Qiagen, Venlo, Netherlands) with following protocol: 95 °C for 3 s, 60 °C for 20 s. Primer sequences for specific Sybr green PCR was performed with human specific primers (Table S3). Taqman PCR primer/probe combinations (Applied Biosystems, Life Technologies, Carlsbad, CA) were used in the *in vitro* osteogenesis assays: RUNX2: Hs00231692_m1; DLX5: Hs00193291_m1; ALP: Hs00758162_m1; OCN: Hs01587814_g1; iBSP: Hs00173720_m1, RANKL: Hs00243522_m1; BMP2: Hs00154192_m1; SPP1: Hs00167093_m1; GAPDH: Hs99999905_m1.

2.7. Phospho protein screening and western blots

The *in vitro* protein phosphorylation signature from hPDCs cultured on CPRM and CPDM scaffolds for 20 h was defined using the Human Phospho-Kinase Antibody Array kit (R&D Systems) according the manufacturer's instructions. Quantification of the resultant blots was carried out using image analysis software (AIDA 1D Evaluation). Protein phosphorylation from *in vivo* samples was analyzed by Western blot. Briefly, the implants were lysed in protein extraction buffer containing 0.3 M PMSF and Protease Inhibition Cocktail (Sigma, Bornem, Belgium). The protein concentration was determined using the Pierce™ BCA Protein Assay Kit (Thermo SCIENTIFIC, Erembodegem, Belgium) and 10 μg loaded onto a NuPAGE 4–12% Bis-Tris gel (Invitrogen, Merelbeke, Belgium) and thereafter transferred to a Polyvinylidene fluoride membrane for further analysis. Primary antibodies were diluted according to the manufacturer's instructions: rabbit monoclonal Phospho-p38 (Thr180/Tyr182), mouse monoclonal Phospho-p44/42 MAPK(Erk1/2) (Thr202/Tyr204) (E10), rabbit monoclonal Phospho-Smad2 (Ser465/467) (138D4), mouse monoclonal Phospho-p53 (Cell Signaling Technology, MA, United States), rabbit polyclonal Phospho-NFκ-β (p105/p50) (Abcam, Cambridge, UK), rabbit polyclonal Phospho-CREB (S133) (R&D Systems, Oxon, UK) and sheep polyclonal dephospho-β-catenin (CTNNB1) (Genway Biotech, San Diego, United States). Glyceraldehyde-3-phosphate dehydrogenase (GAPDH) mouse monoclonal (Abcam, Cambridge UK) was used to assess equal loading of proteins. HRP-conjugated secondary antibodies were used at a dilution of 1:2000 (Jackson, Pennsylvania, United States) and images were developed by a LAS3000 Imaging System (FUJI) following the application of SuperSignal® West Femto reagent (Thermo Scientific, Illnois, United States). Densitometry analysis was performed using Biorad Quantity One software.

2.8. Statistical analysis

Experiments were carried out in triplicate. The error bars represent the standard error of the mean when cells from multiple donors are used. Standard deviations are shown when experiments are performed with the hPDC cell pool ($n = 3$). Statistical comparison between experimental conditions was performed with a Mann–Whitney U test. A p-value $\leq^{\circ}0.05$ was considered as being statistically significant.

3. Results

3.1. Characterization of in vivo bone formation dynamics

CPRM seeded with hPDCs displayed *de novo* bone spicules following 8 weeks of implantation (Fig. 1A). In contrast, CPDM seeded with the same cells did not exhibit bone formation, suggesting that CaP is required for *in vivo* osteogenic differentiation. To determine the time window of osteogenic differentiation *in vivo*, CPDM and CPRM loaded with hPDCs ($n = 3$ donors) were subcutaneously implanted for periods of 2, 8, 18 and 28 days. Within 18 days, the early bone marker Osterix (OSX) and the more mature osteoblast markers Bone Sialo Protein (iBSP) and Osteocalcin (OCN) were upregulated in the CPRM (Fig. 1B). Based on the expression of these three markers, we considered 20 h after seeding, 2 days, 8 days and 18 days as four time points to explore gene expression through microarray analysis. Indeed, the genes of interest (GOI) list revealed a characteristic osteoblast gene signature in CPRM and not in CPDM at 18 days (Fig. 1C). Interestingly, the osteocyte marker Dental Matrix Protein 1 (DMP1), but not Sclerostin or phosphate regulated endopeptidase homolog, X-linked (PHEX) was significantly upregulated (Fig. 1C) indicating the presence of mature osteoblasts but not osteocytes after three weeks of implantation.

To validate the microarray data, gene expression of Osterix (OSX), Osteopontin (OPN), Anoctamin-1 (ANO1), Naked Cuticle 2 (NKD2), Sarcolipin (SLN), and Receptor Activator of Nuclear factor Kappa-B Ligand (RANKL) were verified by Sybr green quantitative PCR (qPCR) using human specific primers. The relative gene expression values measured with qPCR and microarray were comparable in CPRM, but to a lesser extent in CPDM (Fig. 2).

To allow an insight into the biological processes represented by the GOI, gene ontology (GO) analysis was performed (Table 1). GO indicates that distinct processes took place at each time point, commencing with regulation of apoptosis (20 h), followed by positive regulation of transcription and migration (2 days) and proliferation, angiogenesis and osteogenesis at 18 days.

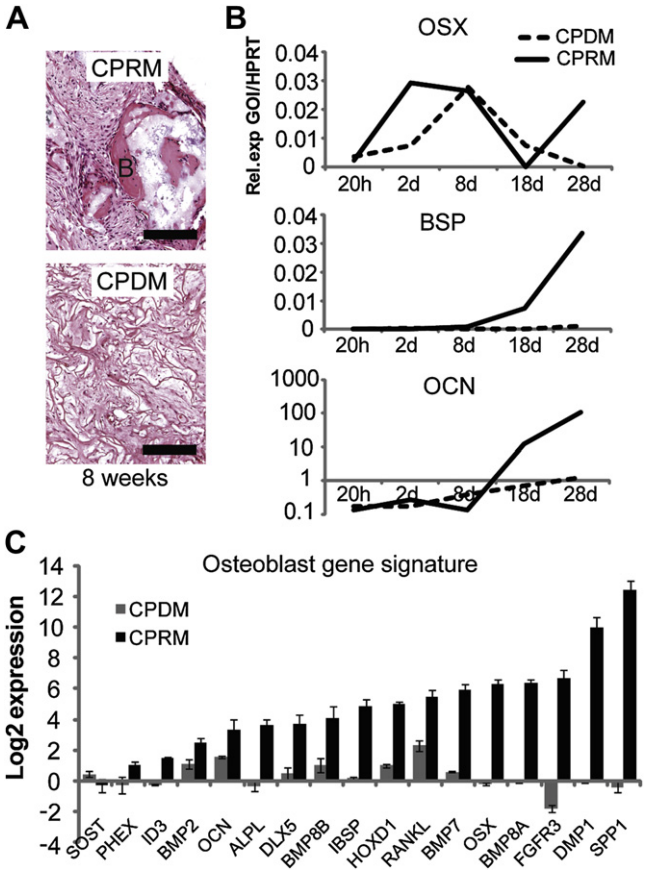

Fig. 1. Osteogenic differentiation occurs within three weeks following implantation in CPRM. A) Histological micrographs of hPDC laden CPRM and CPDM after 8 weeks of subcutaneous implantation (B: bone, H&E staining, bar = 100 μm). B) Average gene expression of Osterix (OSX), Bone Sialo Protein (BSP) and Osteocalcin (OCN) as measured with Taqman PCR ($n = 3$ donors). C) Relative gene expression levels of osteoblast markers at 18 days in CPDM (decalcified Collagraft™) and CPRM (Collagraft™). Gene expression levels are measured with microarray and expressed as $\log_2$ values normalized to culture vessel seeded hPDCs (2D) ($n = 3$ donors, error bar = S.E.M.).

Interestingly, the GOI was enriched for genes associated with Transforming Growth Factor β (TGFβ), Epidermal Growth Factor (EGF) and MAPK signaling. Furthermore, genes related to acute inflammation response were downregulated at this time point. Hence, these data illustrate that the ossification process elicited by hPDCs in CPRM is a sequence of events that results in the progression of the engrafted hPDCs to mature osteoblasts within three weeks of implantation.

3.2. Mapping and validation of CaP activated hub genes

Although informative the GO analysis provides little insight into the mechanisms regulating ectopic bone formation. To decipher the molecular signaling pathways that were specifically activated in CPRM, GOI's were first clustered in Self Organizing Maps (SOMs) (Fig. 3A). SOMs assign genes with comparable temporal expression profiles to the same tile in a 2D plot. Neighboring tiles on the SOM behave very similar throughout the experiment, whereas distant tiles behave in opposite trends. As each tile is color coded according to the average gene expression of the assigned GOI's (blue = low expression, red = high expression), gene expression is visualized into distinct patterns on a heat map which facilitates comparing gene expression of multiple conditions and time points [16]. When comparing the SOMs of CPDM and CPRM, gene expression patterns in the two conditions were similar at 20 h or two days after

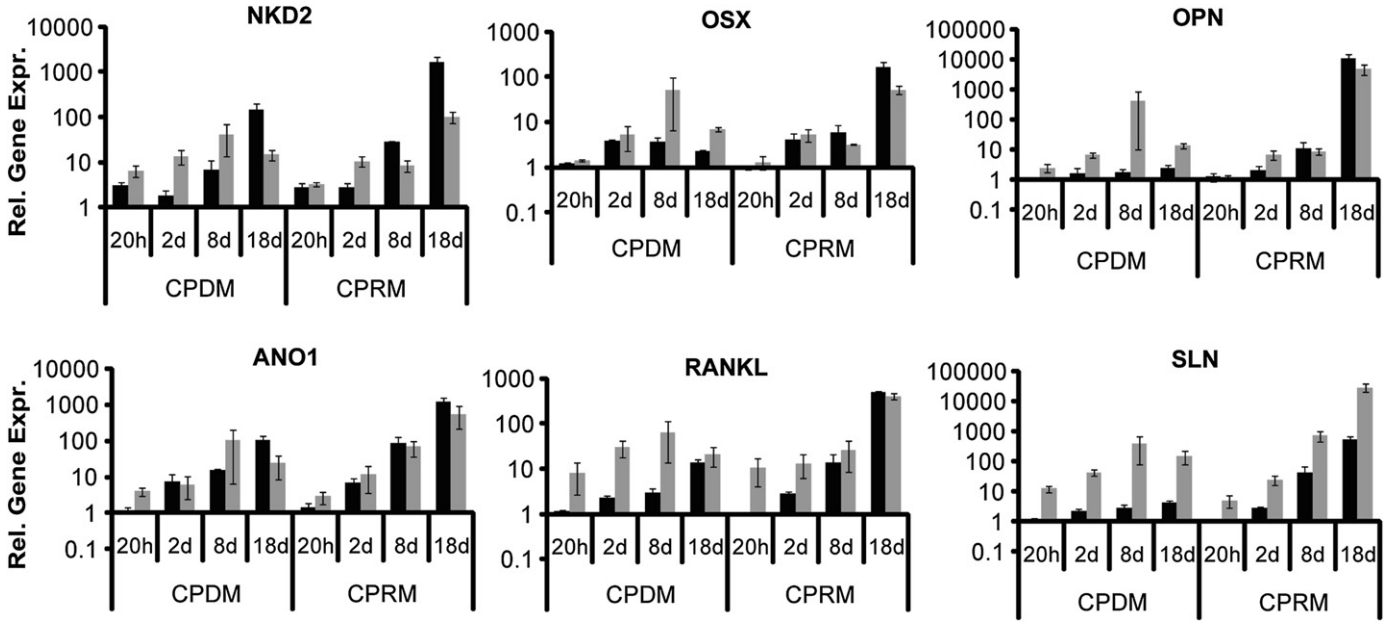

Fig. 2. Validation of microarray gene expression. Microarray gene expression was compared to gene expression levels measured with Sybr green PCR utilizing human specific primers for Anoctamin-1 (ANO1), Naked Cuticle (NKD2), Osterix (OSX), Osteopontin (OPN), Sarcolipin (SLN), and Bone Sialo Protein (BSP). Gene expression is normalized to the housekeeping gene GAPDH. Black bars: microarray expression, gray bars: expression measured with Sybr green PCR ($n = 3$ donors, error bars: S.E.M.).

implantation. In contrast, the gene expression patterns were highly distinct when comparing the SOMs of 20 h after seeding (*in vitro*) with 2 days after implantation (*in vivo*). Interestingly, the SOMs of CPDM at eight days and 18 days resembled the SOMs of CPRM at two and eight days, respectively. Taken together, these data show that gene expression patterns in both matrices underwent similar changes when transferred from an *in vitro* to *in vivo* environment, but upon implantation gene trajectories progressed faster in CPRM as compared to CPDM.

To reduce the number of clusters obtained with the SOM analysis, clusters with similar temporal profiles of the metagenes were grouped into six superclusters (Fig. 3B, Fig. S2). For each supercluster, gene networks were assembled (Table S2) from which hub genes were selected and mapped into a hub gene network connecting the hubs with "direct" and "indirect" gene/protein interactions (Fig. 3C). A number of hub genes known to be involved in bone formation such as β-CATENIN, LEF1, RUNX2, OSX, ALP, BMP7, NOTCH, and HEY1 were upregulated in CPRM (Fig. 3C, red symbols). One hub gene, KITLigand, was downregulated (green symbols) and several hub genes linked to TGFβ (TGFβ1), MAPK (P38, ERK1/2), TNFα (TNFα, IFNγ, IL6, NfkB), EGF (ERBB2, GRB2, EGFR), and P53 signaling (TP53) were not differentially expressed at the gene transcription level (white symbols).

To investigate whether these pathways play a role in the ectopic ossification process, we probed for phosphorylated proteins as a measurement of signal activation. *In vitro*, hPDCs seeded on CPRM

Table 1
Functional Gene Annotation for gene sets which were up or downregulated as compared to the previous time point and differentially expressed between CPRM and CPDM. An EAS score above 1.25 represents a significance level of $p \leq 0.05$ (EAS = Enrichment Association Score from DAVID).

	20 h	EAS	2 days	EAS
Upregulated	Response to peptide hormone stimulus	1.76	Citrullination/Histone H2A	4.92
	Regulation of apoptosis	1.1	Chromatin assembly/DNA packaging	3.89
			Cellular Macromolecular complex assembly	2.9
			Contractile fiber/myofiber	1.72
			Calcium homeostasis	1.65
			Positive regulation of transcription	1.63
			Cell fate commitment	1.27
			Ossification	1.21
			Blood vessel morphogenesis	1.19
	8 days	**EAS**	**18 days**	**EAS**
Upregulated	Ion homeostasis	1.64	Negative regulation of transcription	3.59
	g-protein coupled receptor	1.37	Regulation of ossification	3.55
			Mitosis	3.16
			Protein phosphatase activity	3.14
			Neuron development	2.49
			EGF-like domain	1.94
			Branching morphogenesis of a tube	1.91
			TGF beta/hedgehog signaling	1.88
			MAPK phosphatase activity	1.75
Downregulated	Zinc finger, C2H2-type	3.47	Cell migration	4.25
			Fibrinogen	2.45
			Acute inflammatory response	1.98
			Angiogenesis	1.71

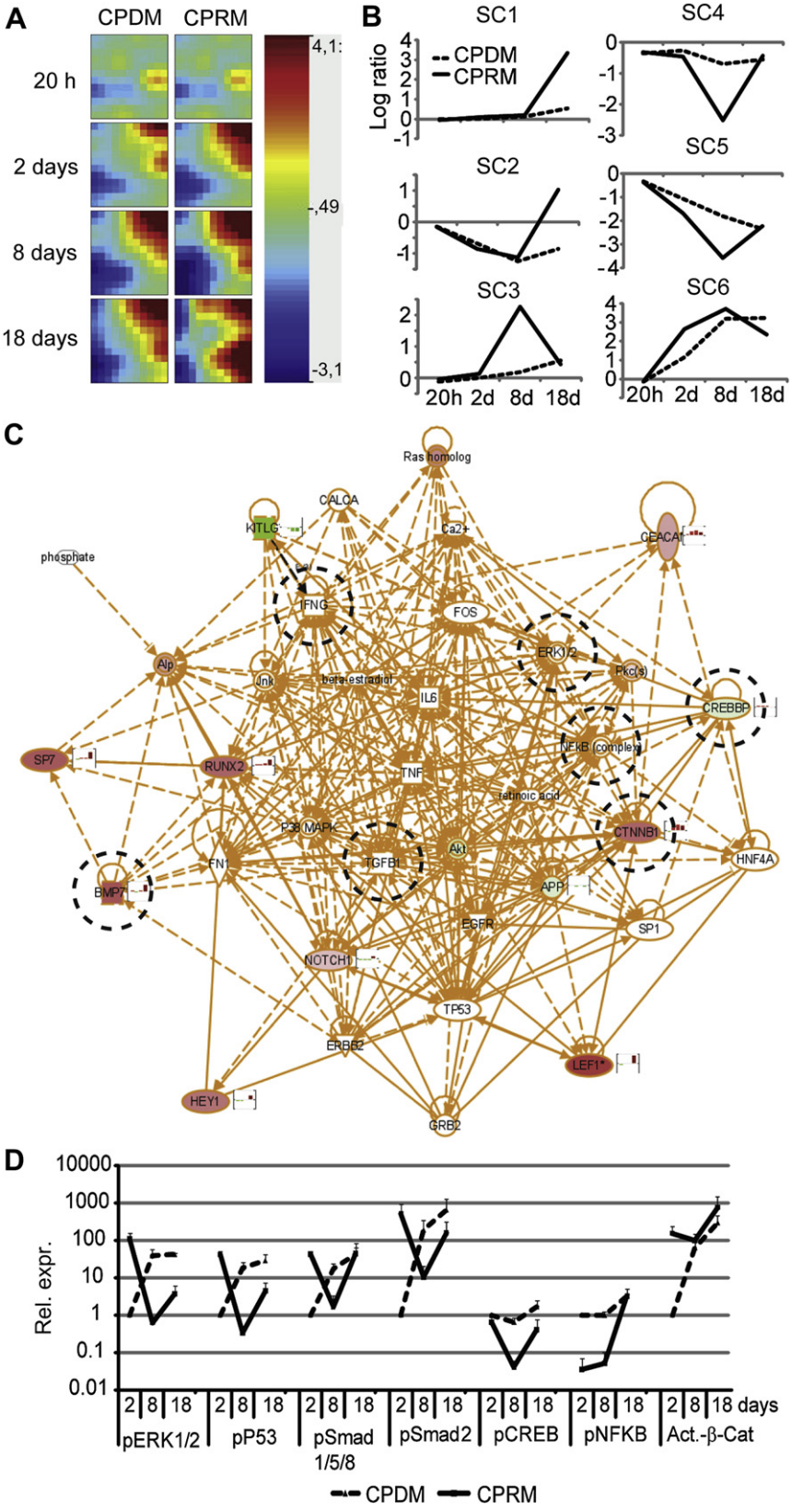

Fig. 3. Mapping and validation of osteogenic hub gene network. A) Self Organizing Maps showing gene expression patterns of GOI at 20 h after seeding and 2, 8 and 18 days after implantation in CPDM and CPRM. Gene expression is normalized to expression in hPDCs seeded on tissue culture plastic for 20 h. B) Average gene expression of co-expressed genes organized in superclusters (SC) plotted over time. Solid line: CPRM, dashed line: CPDM. C) Hub genes from each supercluster are mapped into a single hub gene network. The hub genes are connected with direct (solid lines) and indirect (dashed lines) interactions as determined by Ingenuity Pathway Analysis. Hubs in red are upregulated in CPRM at 18 days post-implantation, hubs in green are downregulated. The encircled hub genes are probed with western blot to validate differential activation between CPRM and CPDM (Fig. S3). D) Quantification of western blots of p-pERK (MAPK signaling), p-p53, p-Smad1/5/8 (BMP signaling), p-Smad2 (TGFβ signaling), p-CREB (cAMP and EGF signaling), p-NFκB (TNFα/NFκB signaling), and p-β-catenin (β-catenin/Wnt signaling). Densitometry values are normalized to GAPDH. For all time points, fold increase is compared to the expression in CPDM at two days ($n = 3$ donors, error bar: S.E.M.).

displayed higher levels of p-CREB (S133) and p-P53 (S392) and lower levels of pERK1/2 (T202/Y204, T185/Y187) as compared to cells seeded on CPDM (Fig. S3A). *In vivo*, p-Erk1/2, p-P53, p-Smad1/5/8, p-Smad2 and p-CREB displayed similar biphasic temporal profiles in CPRM, with a high expression two days and 18 days after implantation (Fig. 3D, S3B). Activated beta catenin showed an analogous profile to p-Erk, p-P53 and p-Smads in CPDM. All tested phosphorylated proteins that were identified in the hub gene network, displayed differential expression between CPDM and CPRM. These data validated our network and demonstrated that mapping a hub gene network starting from gene expression data is a compelling approach to predict differential activation of signaling pathways at the protein level.

3.3. Development of an osteogenic growth factor cocktail based on hub gene activation

Since a specific set of hub genes was identified, we questioned if activation of the identified signaling pathways in hPDCs would promote osteogenic differentiation *in vitro*. Utilizing a "leave-one-factor-out" strategy, we aimed to identify key factors that stimulate proliferation and differentiation of hPDCs *in vitro*. Based on the hub gene network, we selected TNFα, IL6, EGF, TGFβ1, Wnt3A ligands along with calcium and phosphate ions as factors to induce osteogenic differentiation. Dexamethasone based osteogenic medium (OM) was included due to its status as the gold standard for *in vitro* osteogenic differentiation [17]. OM supplemented with all factors was used as a reference to evaluate the impact of a single factor, after exclusion from the cocktail, on proliferation, ALP positivity or gene expression. Negative regulation of a metric in absence of one factor indicated the importance of that factor for that metric. Following this reasoning, we identified OM and TGFβ1 as strong inducers of proliferation and ALP expression of hPDCs (Fig. 4A and B). Interestingly, OM promoted ALP expression (Fig. S4A) but reduced basal expression levels of later bone markers, iBSP, SPP1 and RANKL (Fig. S4B). These data indicated that OM interfered with the progression of an osteoprogenitor to a mature osteoblast.

To overcome the inhibitory effect of OM, we explored a two stage protocol wherein hPDCs were treated with OM and TGFβ1 for 6 days, followed by growth medium supplemented with six factors (Ascorbic Acid, TNFα, IL6, EGF, Ca, Pi) minus one factor for 4 days. Ascorbic acid was included in the cocktail due to its stimulatory effect on ALP activity (Fig. S4C) and mineralization (Fig. S4D) *in vitro*. Removal of TNFα resulted in a significant increase in gene expression levels of OSX, iBSP and OCN, thus TNFα was omitted from the growth factor cocktail for later experiments (Fig. 4C). Furthermore, reducing the concentration of calcium and phosphate ions from 6 mM to 4 mM to 3 mM and 2 mM respectively, upregulated gene expression of RUNX2, OSX, SPP1, iBSP (Fig. 4D).

To investigate whether a two stage protocol resulted in enhanced osteogenic differentiation *in vitro*, as compared to a single stage protocol, hPDCs from four different donors were treated with OM/TGFβ1 for 6 days followed by GM/Asc. Ac./EGF/IL6/CaP for 4 days. As a control, hPDCs were treated with stimulation medium of the first stage (OM and TGFβ1) or the second stage (GM supplemented with Asc. Ac., EGF, IL6, Ca/Pi) for 10 days. Surprisingly, gene expression levels for several bone markers (DLX5, BMP2, iBSP, OCN and RANKL) were increased when treated with the second stage growth factor mix only as compared to the two stage protocol (Fig. 4E). These data suggested that stimulation with a growth factor/ion cocktail (GFC) medium containing Asc. Ac., IL6, EGF, TGFβ1, calcium and phosphate ions (Table S4) for 10 days, was optimal for enhancing osteogenic gene expression.

3.4. Evaluation of osteogenic growth factor cocktail

To test the efficacy of the GFC, hPDCs from four donors were treated with the GFC for 10 days and proliferation (Fig. 5A) and osteogenic differentiation (Fig. 5B) were compared to hPDCs treated with OM. Human PDCs treated with the GFC underwent 7 (SEM: ±0.1) population doublings, whereas hPDCs in OM reached 4.8 (SEM: ±0.2) population doublings after 10 days. Interestingly, gene expression of COL1 and ALP (Fig. 5B) were comparable in OM and GFC treated cells. In contrast, mRNA levels of other bone markers characteristic for early (DLX5, OSX, RUNX2, and BMP2), intermediate (SPP1, BSP) and late (RANKL and OCN) stages of osteoblast differentiation were significantly upregulated in GFC treated cells compared to OM treated cells (Fig. 5B).

In order to determine whether pre-treatment of hPDCs with the GFC could enhance ectopic bone formation *in vivo*, hPDCs were seeded on CPDM or CPRM scaffolds, pre-treated with GM or GFC for 10 days and subcutaneously implanted in nude mice for 8 weeks. Whereas GFC pre-treatment could not rescue bone formation in CPDM scaffolds (data not shown), a 6-fold increase of *de novo* bone tissue was measured in hPDC laden CPRM scaffolds as compared to the same implants pre-cultured in GM (Fig. 5C). CPRM scaffolds incubated in GFC containing medium prior to implantation did not show any signs of bone formation (Fig. 5C).

4. Discussion

The identification of signaling cascades/hub genes that are triggered in progenitor cells by CaP scaffolds is an essential step in understanding the mechanism of cellular activation/differentiation that culminates in bone formation. Although it has been proposed that cellular differentiation can be understood, and replicated, by specifically targeting hub genes that control tissue forming signaling cascades during embryonic organogenesis [18], a number of differences exist in the postnatal setting. For example, the release of inflammatory cytokines and influx of immune cells and clotting factors by ruptured blood vessels, which occurs after trauma, is unseen during development. By comparing gene expression postnatally in a tissue forming condition (CPRM) versus loss of function condition (CPDM), we show that *in vivo* molecular processes associated with CaP-driven bone formation can be identified and used to develop culture conditions that promote osteogenesis of human progenitors.

The mechanism by which CaP exerts its osteoinductive effect on progenitor populations is unclear [19]. It has been suggested that endogenous BMPs secreted by the engrafted cells bind to CaP and activate BMP signaling which subsequently drives osteoinduction [20]. Indeed, it has recently been shown that Ca^{2+} upregulates gene transcription of BMP2 in human MSCs [12] and hPDCs [9] *in vitro*. This finding was corroborated herein, as BMP2 gene expression levels were robustly elevated in CPRM *in vivo* and *in vitro* upon treatment with the GFC, thus further supporting a central role for BMP2 in CaP-mediated osteogenesis. However, our data also indicate that many signaling pathways such as EGF, TGFβ, β-catenin and NFκB are differentially activated in CPRM versus CPDM, demonstrating that the mechanism of osteoinduction in CaP scaffolds is more complex than activation of BMP signaling alone. Interestingly, gene expression of the GOI were regulated similarly in both scaffolds upon *in vivo* implantation, but the progression of the gene dynamics was faster in CPRM as compared to CPDM, a finding which is reminiscent of the Regional Accelerated Phenomenon during fracture healing [21]. These data support the hypothesis that the wound healing response induced by implanting the cell-seeded scaffolds may contribute to the activation of osteoinductive gene networks which are mediated by CaP.

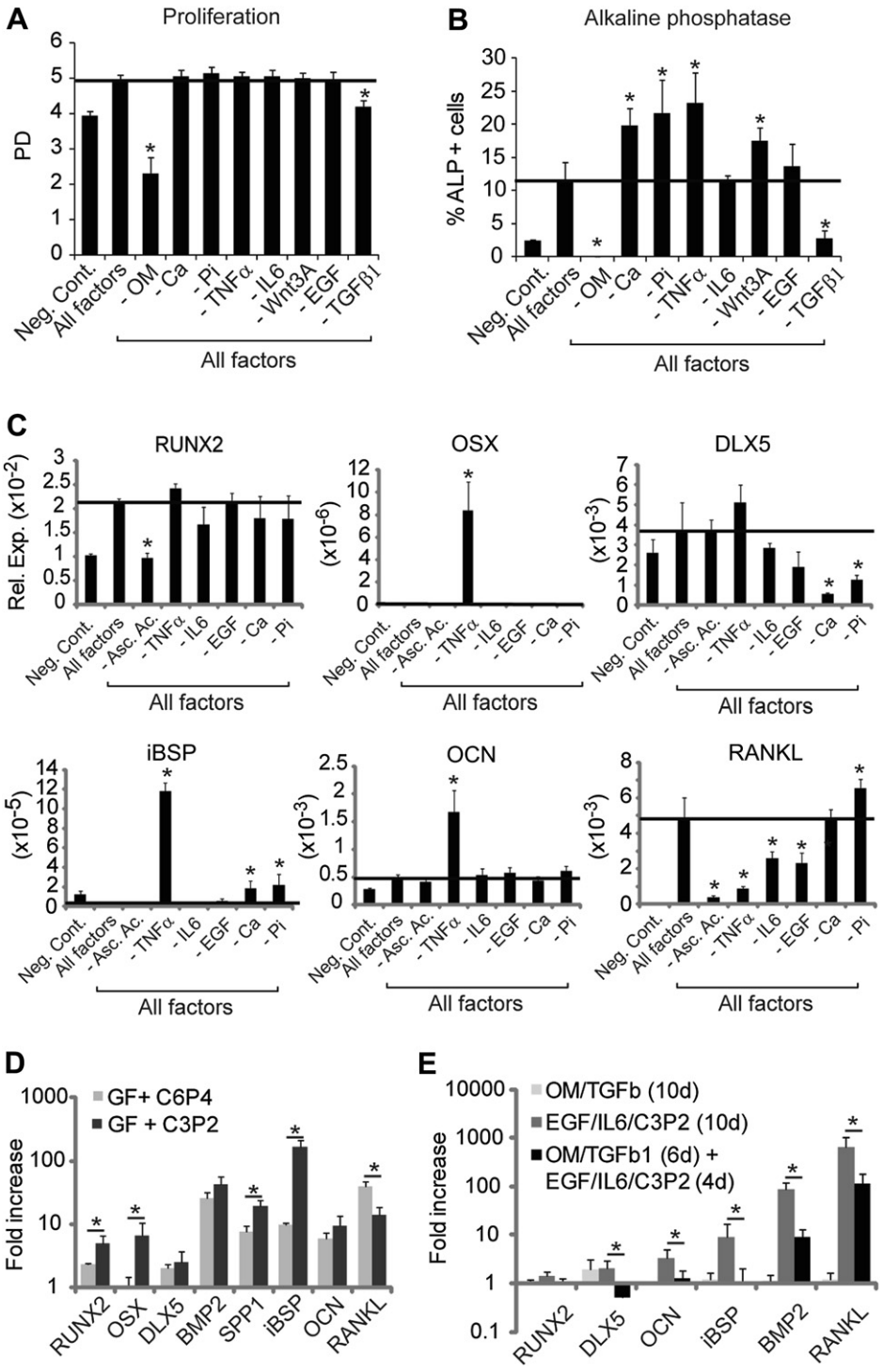

Fig. 4. Development of an osteogenic growth factor cocktail. A) Identification of factors that drive proliferation of hPDCs. A cell pool of hPDCs was either treated with growth medium (GM, negative control), medium containing eight factors (all factors) or medium containing eight minus one factor for 8 days. The factors are osteogenic medium (OM), calcium ions (Ca, 6 mM), phosphate ions (Pi, 4 mM), TNFα (50 ng/ml), IL6 (10 ng/ml), Wnt3A (50 ng/ml), EGF (20 ng/ml), and TGFβ1 (10 ng/ml). Proliferation is expressed as population doublings and was measured after 8 days of stimulation ($n = 3$, error bar: standard deviation). The horizontal line is a reference line set on the proliferation in the "all factor" condition. B) Identification of factors that drive alkaline phosphatase activity in hPDCs. Same experimental design as in A. C) Identification of factors involved in osteoblast maturation. hPDCs were treated with OM and TGFβ1 for 6 days, followed by stimulation with GM (negative control), GM containing six factors or GM supplement with six minus one factor for 4 days. The factors are ascorbic acid (Asc. Ac.), TNFα, IL6, EGF, Ca and Pi. To evaluate osteoblast maturation, gene expression of RUNX2, OSX, DLX5, iBSP, OCN and RANKL is measured with Taqman PCR. Gene expression is normalized to GAPDH and displayed as 2^{-dCT} ($n = 3$, error bars: standard deviation). D) Gene expression of osteoblast markers in hPDCs treated with OM/TGFβ1 for one week followed GM supplemented with ascorbic acid, EGF, IL6, Ca (6 mM), and Pi (4 mM) (GF + C6P4) or the same mix with reduced Ca (3 mM) and Pi (2 mM) ions (GF + C3P2). Gene expression is expressed as fold increase as compared to hPDCs cultured in GM ($n = 3$, error bars: standard deviations, $^*p \leq 0.05$, Mann–Whitney *U* test). E) Gene expression of osteoblast markers in hPDCs treated with OM/TGFβ1 or GM supplemented with ascorbic acid, EGF, IL6, C3P2 for 10 days or sequential stimulation with OM/TGFβ1 for 6 days followed by GM supplemented with ascorbic acid, EGF, IL6, C3P2 for 4 days. Gene expression is expressed as fold increase as compared to hPDCs cultured in OM/TGFβ1 ($n = 3$, error bars: standard deviations, $^*p \leq 0.05$, Mann–Whitney *U* test).

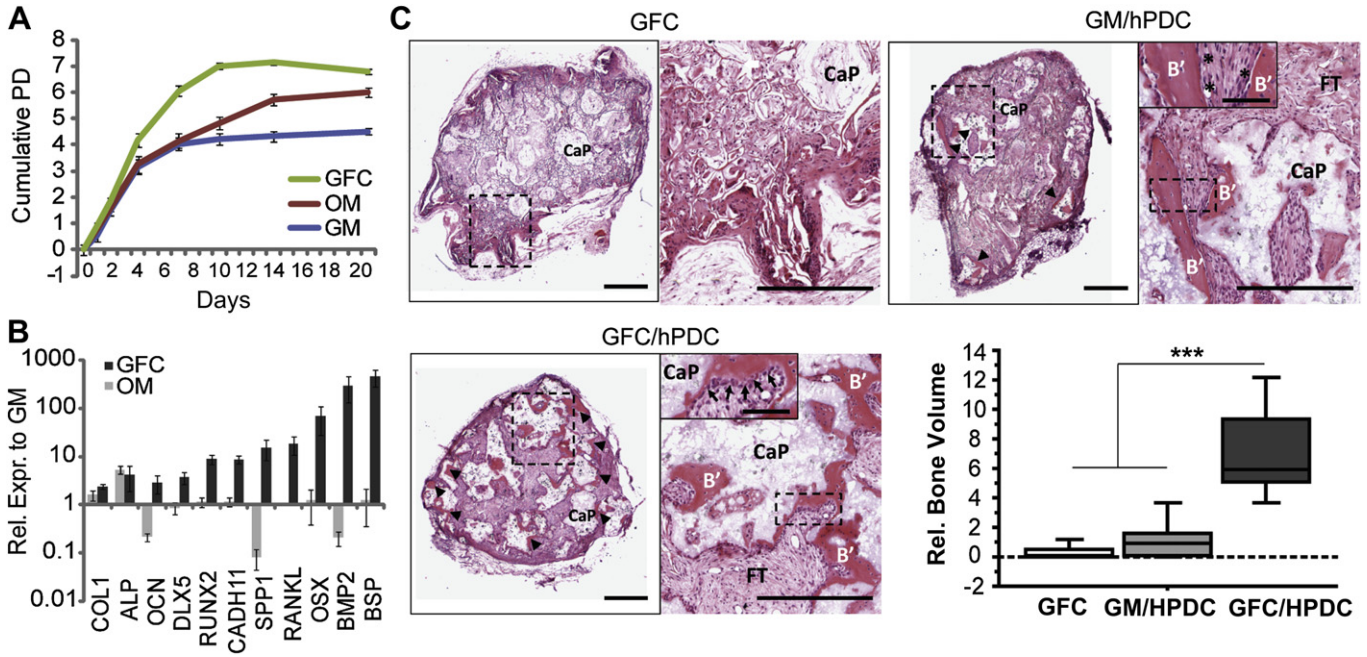

Fig. 5. Stimulation of hPDCs with TGFb, EGF, IL6, Asc. Ac., calcium and phosphate ions promotes osteogenesis *in vitro* and *in vivo*. A) Proliferation, expressed as cumulative population doublings, of hPDCs treated with the growth factor cocktail (GFC), OM and GM. B) Relative gene expression of bone markers of hPDCs after treatment with OM and GFC for 11 days. Gene expression is normalized to the gene expression in the GM condition (CADH11 = osteoblast specific cadherin 11, SPP1 = osteonectin, $n = 4$ donors, bar: S.E.M.). C) Hematoxylin/eosin staining of CPRM implants eight weeks after implantation. CPRMs were incubated in GM containing the GFC (GFC) or seeded with hPDCs and incubated in GM (GM/hPDC) or GM containing the GFC (GFC/hPDC) for 10 days prior to implantation. In the absence of cells, treatment with the GFC did not result in the formation of any bone. In contrast, sporadic bone spicules (B′ and black arrow heads) were observed in the GM/hPDC condition whereas all CaP granules were surrounded by growing bone spicules in the GFC/hPDC implants. Higher magnification (inset of right panel) shows that bone spicules in GM/hPDC implants are aligned by a few fibroblast like lining cells (* Inset) whereas large quantities of cuboidal osteoblast like cells associated with bone growth are found adjacent to *de novo* bone in the GFC/hPDC condition (black arrows, Inset). Histomorphometric analysis revealed a 6 fold increase in bone formation following pre-treatment of hPDCs with the GF cocktail when compared to the GM treated hPDC condition. (B′ = bone, FT = fibrous tissue, $n = 3$; Statistical significance: $^{***}p < 0.001$ ANOVA; Scale bars: left panel = 500 μm; right panel = 200 μm; inset = 50 μm; dashed boxes indicate areas of higher magnification).

During postnatal tissue repair, the wound healing response is characterized by an initial phase of inflammation impacting differentiation and tissue formation. Shortly after bone injury, pro-inflammatory cytokines such as IL6, IFNγ and TNFα, are highly expressed and regulate the initiation and remodeling phase of fracture healing [22,23]. The same set of pro-inflammatory cytokines along with developmental signaling pathways such as TGFβ, BMP and EGFR were mapped in our hub gene network. This was an unexpected finding since both CPDM and CPRM were implanted in a wound environment. It may be speculated that CaP and pro-inflammatory cytokines regulate the same target genes, perhaps through modulation of CREB/cAMP and P53 pathways. The observation that the phosphorylation dynamics of ERK, P53, Smad1/5/8 and Smad2 in CPRM follow a similar biphasic pattern as phosphorylated CREB supports this hypothesis. However, in the absence of CaP, phosphorylation dynamics of ERK, P53, Smad1/5/8 and Smad2 correlated with the dynamics of activated beta catenin and not p-CREB. In fact, independent of the scaffold used, high levels of pERK, p-53, p-Smad1/5/8 and p-Smad2 coincided with increased expression of p-CREB and activated beta catenin; suggesting that activation of both signaling pathways may be required for the initiation of ectopic bone formation. In agreement with our data, prolonged activation of the cAMP pathway by either dibutryl-cAMP [24,25] or forskolin [26] has been shown to stimulate *in vitro* and *in vivo* osteogenesis in human bone marrow cells. However, this beneficial effect is dependent on the dose and duration of the stimulus [27].

The key role that the humoral environment plays in the early phases of CaP mediated osteoinduction was revealed by the finding that inflammatory signaling was captured in the hub gene network. The contribution of the host environment to later stages of the ossification process has previously been reported, with direct host cell contribution to the vascularization [28] and bone tissue formation processes [14,29]. Examination of paracrine signaling between the implanted cells and host cells may provide further clues to the nature of their co-operation in the ectopic bone formation model. One viable approach to address this would be by genetic labeling of the host and engrafted cells so identification of the origin of each cell during each stage of ectopic bone formation would be possible [28].

It was hypothesized that by mimicking the CaP and host environment *in vitro*, through the stimulation of the identified signaling pathways, an enhanced osteogenic differentiation and *in vivo* performance may be achieved. Through a 'leave-one-factor-out' strategy, previously utilized to reprogram fibroblasts to pluripotent stem cells [30], it was possible to develop a GFC, containing Asc. Ac., IL6, EGF, TGFβ1, $Ca^{2}+$ and Pi, that could orchestrate *in vitro* osteogenic differentiation. Remarkably, *in vitro* preconditioning of hPDCs with the GFC resulted in a 6-fold increase of *de novo* bone tissue *in vivo*. In contrast, we have previously reported that while pre-treatment of hPDCs with OM or with $Ca^{2}+$ and Pi improved *in vitro* osteogenic differentiation, it subsequently abrogated *in vivo* bone formation [10]. This may indicate that Ca^{2+} and Pi or OM treatment alone do not allow a stable osteoblastic cell state before implantation. Indeed, dexamethasone, a synthetic glucocorticoid present in OM, has been shown to down regulate gene transcription of the late stage osteogenic differentiation marker OCN, therefore inhibiting osteoblast maturation [31–33]. Interestingly, even though Ca^{2+} and Pi are present in our GFC, the addition of other factors overrides its inhibitory effect on *in vivo* osteogenesis.

This is likely to be due to positive regulation of a wide range of osteogenic markers, and also by preventing down regulation of Collagen Type I gene expression [10], a marker predictive for *in vivo* bone formation [34]. Hence, in conjunction with these previous studies, our data emphasize the impact of *in vitro* culture conditions to control the *in vivo* outcome of human progenitor cells in combination with clinically relevant biomaterials.

Notably, pre-treatment of hPDCs with soluble factors did not replace the CPRM condition as no ossified tissue was found in GFC pre-treated CPDM scaffolds. Therefore, other cues related to matrix–cell interactions whether dictated by matrix stiffness [35], matrix topography [36], collagen anchoring [37], the biophysical properties of CaP [38], or scaffold architecture [39] may need to be incorporated to mimic CaP mediated osteoinduction.

5. Conclusion

Although much research has been conducted on cell differentiation to develop cell/biomaterial based tissue engineered products, the influence of the environment upon the implants after implantation has been largely neglected. The strategy employed herein highlights the importance of this environment, in combination with materials properties, for cell activation and subsequent tissue formation. It is proposed that a better understanding of the molecular and cellular mechanisms surrounding this phenomenon will serve to allow the creation of biologically functional biomaterials [40] with defined cell-specific properties for regenerative strategies.

Conflict of interest

All authors have no conflict of interest.

Acknowledgments

The authors are grateful to Carla Geeroms and Kathleen Bosmans for excellent technical assistance. This work was supported by the Research Foundation – Flanders (grant number G.0590.09) Stem Cell Institute of Leuven—KU Leuven and National Institutes of Health (grant numbers GM60692, EB 00262). J.E. and S.R. are postdoctoral fellows of the Research Foundation – Flanders (FWO). J.B. is a Ph.D. fellow of the Innovation by Science and Technology (IWT). This work is part of Prometheus, the Leuven Research & Development Division of Skeletal Tissue Engineering of the KU Leuven (www.kuleuven.be/prometheus).

Appendix A. Supplementary data

Supplementary data related to this article can be found at http://dx.doi.org/10.1016/j.biomaterials.2013.03.011.

References

[1] Haynesworth SE, Goshima J, Goldberg VM, Caplan AI. Characterization of cells with osteogenic potential from human marrow. Bone 1992;13:81–8.
[2] Hicok KC, Du Laney TV, Zhou YS, Halvorsen YD, Hitt DC, Cooper LF, et al. Human adipose-derived adult stem cells produce osteoid in vivo. Tissue Eng 2004;10:371–80.
[3] Dell'Accio F, De Bari C, Luyten FP. Microenvironment and phenotypic stability specify tissue formation by human articular cartilage-derived cells in vivo. Exp Cell Res 2003;287:16–27.
[4] De Bari C, Dell'Accio F, Tylzanowski P, Luyten FP. Multipotent mesenchymal stem cells from adult human synovial membrane. Arthritis Rheum 2001;44:1928–42.
[5] Nakahara H, Goldberg VM, Caplan AI. Culture-expanded human periosteal-derived cells exhibit osteochondral potential in vivo. J Orthop Res 1991;9:465–76.
[6] Langer R, Vacanti JP. Tissue engineering. Science 1993;260:920–6.
[7] Lenas P, Moos M, Luyten FP. Developmental engineering: a new paradigm for the design and manufacturing of cell-based products. Part I: from three-dimensional cell growth to biomimetics of in vivo development. Tissue Eng Part B Rev 2009;15:381–94.
[8] Jung GY, Park YJ, Han JS. Effects of HA released calcium ion on osteoblast differentiation. J Mater Sci Mater Med 2010;21:1649–54.
[9] Chai YC, Roberts SJ, Schrooten J, Luyten FP. Probing the osteoinductive effect of calcium phosphate by using an in vitro biomimetic model. Tissue Eng Part A 2011;17:1083–97.
[10] Chai YC, Roberts SJ, Desmet E, Kerckhofs G, van Gastel N, Geris L, et al. Mechanisms of ectopic bone formation by human osteoprogenitor cells on CaP biomaterial carriers. Biomaterials 2012;33:3127–42.
[11] Colnot C. Skeletal cell fate decisions within periosteum and bone marrow during bone regeneration. J Bone Miner Res 2009;24:274–82.
[12] Barradas AM, Fernandes HA, Groen N, Chai YC, Schrooten J, van de PJ, et al. A calcium-induced signaling cascade leading to osteogenic differentiation of human bone marrow-derived mesenchymal stromal cells. Biomaterials 2012;33:3205–15.
[13] Liu Y, Cooper PR, Barralet JE, Shelton RM. Influence of calcium phosphate crystal assemblies on the proliferation and osteogenic gene expression of rat bone marrow stromal cells. Biomaterials 2007;28:1393–403.
[14] Eyckmans J, Roberts SJ, Schrooten J, Luyten FP. A clinically relevant model of osteoinduction: a process requiring calcium phosphate and BMP/Wnt signalling. J Cell Mol Med 2010;14:1845–56.
[15] Huang dW, Sherman BT, Lempicki RA. Systematic and integrative analysis of large gene lists using DAVID bioinformatics resources. Nat Protoc 2009;4:44–57.
[16] Eichler GS, Huang S, Ingber DE. Gene Expression Dynamics Inspector (GEDI): for integrative analysis of expression profiles. Bioinformatics 2003;19:2321–2.
[17] Jaiswal N, Haynesworth SE, Caplan AI, Bruder SP. Osteogenic differentiation of purified, culture-expanded human mesenchymal stem cells in vitro. J Cell Biochem 1997;64:295–312.
[18] Murry CE, Keller G. Differentiation of embryonic stem cells to clinically relevant populations: lessons from embryonic development. Cell 2008;132:661–80.
[19] Chai YC, Carlier A, Bolander J, Roberts SJ, Geris L, Schrooten J, et al. Current views on calcium phosphate osteogenicity and the translation into effective bone regeneration strategies. Acta Biomater 2012;8:3876–87.
[20] Ripamonti U. Osteoinduction in porous hydroxyapatite implanted in heterotopic sites of different animal models. Biomaterials 1996;17:31–5.
[21] Frost HM. The regional acceleratory phenomenon: a review. Henry Ford Hosp Med J 1983;31:3–9.
[22] Gerstenfeld LC, Cullinane DM, Barnes GL, Graves DT, Einhorn TA. Fracture healing as a post-natal developmental process: molecular, spatial, and temporal aspects of its regulation. J Cell Biochem 2003;88:873–84.
[23] Mountziaris PM, Mikos AG. Modulation of the inflammatory response for enhanced bone tissue regeneration. Tissue Eng Part B Rev 2008;14:179–86.
[24] Siddappa R, Martens A, Doorn J, Leusink A, Olivo C, Licht R, et al. cAMP/PKA pathway activation in human mesenchymal stem cells in vitro results in robust bone formation in vivo. Proc Natl Acad Sci U S A 2008;105:7281–6.
[25] Doorn J, van de PJ, van Leeuwen JP, Groen N, van Blitterswijk CA, de Boer J. Pro-osteogenic trophic effects by PKA activation in human mesenchymal stromal cells. Biomaterials 2011;32:6089–98.
[26] Doorn J, Siddappa R, van Blitterswijk CA, de Boer J. Forskolin enhances in vivo bone formation by human mesenchymal stromal cells. Tissue Eng Part A 2012;18:558–67.
[27] Siddappa R, Doorn J, Liu J, Langerwerf E, Arends R, van Blitterswijk C, et al. Timing, rather than the concentration of cyclic AMP, correlates to osteogenic differentiation of human mesenchymal stem cells. J Tissue Eng Regen Med 2010;4:356–65.
[28] Tasso R, Fais F, Reverberi D, Tortelli F, Cancedda R. The recruitment of two consecutive and different waves of host stem/progenitor cells during the development of tissue-engineered bone in a murine model. Biomaterials 2010;31:2121–9.
[29] Roberts SJ, Geris L, Kerckhofs G, Desmet E, Schrooten J, Luyten FP. The combined bone forming capacity of human periosteal derived cells and calcium phosphates. Biomaterials 2011;32:4393–405.
[30] Takahashi K, Yamanaka S. Induction of pluripotent stem cells from mouse embryonic and adult fibroblast cultures by defined factors. Cell 2006;126:663–76.
[31] Lian JB, Shalhoub V, Aslam F, Frenkel B, Green J, Hamrah M, et al. Species-specific glucocorticoid and 1,25-dihydroxyvitamin D responsiveness in mouse MC3T3-E1 osteoblasts: dexamethasone inhibits osteoblast differentiation and vitamin D down-regulates osteocalcin gene expression. Endocrinology 1997;138:2117–27.
[32] Viereck V, Siggelkow H, Tauber S, Raddatz D, Schutze N, Hufner M. Differential regulation of Cbfa1/Runx2 and osteocalcin gene expression by vitamin-D3, dexamethasone, and local growth factors in primary human osteoblasts. J Cell Biochem 2002;86:348–56.
[33] Roberts SJ, Chen Y, Moesen M, Schrooten J, Luyten FP. Enhancement of osteogenic gene expression for the differentiation of human periosteal derived cells. Stem Cell Res 2011;7:137–44.
[34] De Bari C, Dell'Accio F, Karystinou A, Guillot PV, Fisk NM, Jones EA, et al. A biomarker-based mathematical model to predict bone-forming potency of

human synovial and periosteal mesenchymal stem cells. Arthritis Rheum 2008;58:240–50.
[35] Engler AJ, Sen S, Sweeney HL, Discher DE. Matrix elasticity directs stem cell lineage specification. Cell 2006;126:677–89.
[36] Dalby MJ, Gadegaard N, Tare R, Andar A, Riehle MO, Herzyk P, et al. The control of human mesenchymal cell differentiation using nanoscale symmetry and disorder. Nat Mater 2007;6:997–1003.
[37] Trappmann B, Gautrot JE, Connelly JT, Strange DG, Li Y, Oyen ML, et al. Extracellular-matrix tethering regulates stem-cell fate. Nat Mater 2012;11:642–9.
[38] Habibovic P, Sees TM, van den Doel MA, van Blitterswijk CA, de Groot K. Osteoinduction by biomaterials–physicochemical and structural influences. J Biomed Mater Res A 2006;77:747–62.
[39] Scaglione S, Giannoni P, Bianchini P, Sandri M, Marotta R, Firpo G, et al. Order versus disorder: in vivo bone formation within osteoconductive scaffolds. Sci Rep 2012;2:274.
[40] Mieszawska AJ, Kaplan DL. Smart biomaterials – regulating cell behavior through signaling molecules. BMC Biol 2010;8:59.

List of abbreviations

ALP: alkaline phosphatase
ANO1: Anoctamin-1
Asc Ac: ascorbic acid
BMP: Bone Morphogenetic Protein
BSP: Bone Sialo Protein
Ca^{2+}: calcium ions
CaP: calcium phosphate
CPDM: calcium phosphate depleted matrix
CPRM: calcium phosphate rich matrix
CREB: cAMP responsive element binding protein
CTNNB1: β-catenin
DLX5: Distal-Less Homeobox 5
DMP1: Dental Matrix Protein 1
EGF: Epidermal Growth Factor
ERK: extracellular signal-regulated kinases
GAPDH: glyceraldehyde-3-phosphate dehydrogenase
GFC: growth factor cocktail
GM: growth medium
GO: gene ontology
GOI: genes of interest
hPDCs: human periosteum derived cells
IL6: interleukin 6
MAPK: mitogen-activated protein kinase
NFkB: Nuclear Factor kappa-B
NKD2: Naked Cuticle 2
OCN: osteocalcin
OPN: osteopontin
OSX: osterix
PHEX: phosphate regulated endopeptidase homolog, X-linked
Pi: phosphate ions
RANKL: Receptor Activator of Nuclear factor Kappa-B Ligand
RUNX2: Runt related Transcription Factor 2
SLN: Sarcolipin
SOM: Self Organizing Map
SPP1: Secreted Phospho Protein 1/Osteonectin
TGFβ: Transforming Growth Factor Beta
TNFα: Tumor Necrosis Factor Alpha